CHEMISTRY OF MATERIALS

ARTICLE

pubs.acs.org/cm

Influence of Complex-Formation Equilibria on the Temporal Persistence of Cysteinate-Functionalized CdSe Nanocrystals in Water

Jared S. Baker, Jeremy S. Nevins, Kathleen M. Coughlin, Luis A. Colón,* and David F. Watson*

Department of Chemistry, University at Buffalo, The State University of New York, Buffalo, New York 14260-3000, United States

Supporting Information

ABSTRACT: We have characterized the persistence and degradation of magic-sized CdSe nanocrystals (NCs) after their removal from the original reaction mixture and dispersion into basic aqueous solutions. Such studies are important given the myriad potential applications of semiconductor NCs and ongoing efforts to characterize the properties and reactivity of monodisperse suspensions of intact NCs. Correlated challenges are to elucidate the mechanisms by which NCs degrade and to establish conditions under which NCs persist. Our CdSe NCs degraded after dilution into aqueous NaOH, resulting in red-shifted excitonic absorption bands and eventual flocculation. Dilution of NCs into basic aqueous solutions of cysteinate resulted in degradation via a different mechanism with an absence of flocculation; kinetics varied with concentration of cysteinate. The chemical fate of NCs after dilution into basic aqueous solutions containing both Cd^{2+} and cysteinate varied with the cysteinate-to-Cd^{2+} molar ratio, which determined the relative solute mole fractions of various Cd^{2+}−cysteinate complexes. CdSe NCs persisted on long time scales only when dispersed in solutions containing $[Cd(cysteinate)_3]^{4-}$. We present equilibria to account for the observed spectral changes after dilution of CdSe into various basic media. Cadmium(II)−cysteinate complex-formation equilibria influenced the temporal persistence of the NCs; the pathway through which CdSe NCs degraded depended on the concentration of free, uncoordinated cysteinate. Our findings indicate that solution-phase chemistry can determine whether NCs remain intact upon removal from their original reaction mixtures.

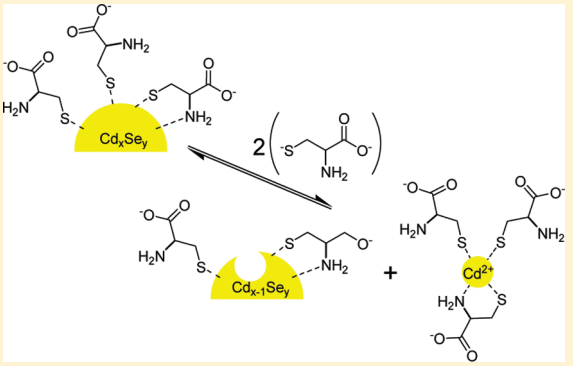

KEYWORDS: magic-sized clusters, semiconductor nanocrystals, quantum dots, cadmium selenide, cysteine, persistence and degradation

INTRODUCTION

Considerable attention has been devoted to cadmium chalcogenide nanocrystals (NCs) over the past three decades, due in part to their unique size-tunable properties, which have enabled applications such as biological labeling,[1,2] generation of light,[3] and the harvesting and conversion of solar energy.[4] Much research has focused on fine-tuning syntheses to yield NCs of desired compositions with tunable sizes and narrow size distributions. Well-established syntheses involving metal−organic precursors and organic capping agents yield hydrophobic NCs.[3,5−7] For applications in aqueous environments, further ligand exchange is required to engender aqueous dispersibility of such NCs.[5,8] As a result, there has been significant interest in the development of fully aqueous syntheses of water-dispersible cadmium chalcogenide NCs.[9−27] Park and co-workers recently reported a promising approach, which utilizes cysteinate (Cys) as a capping agent and yields ultrasmall CdSe NCs with diameters less than 2 nm.[16−18] The optical properties of these NCs are consistent with those of thermodynamically stable "magic-sized" clusters that exhibit quantized growth, narrow size distributions, and narrow excitonic absorption bands.[28] Recently, magic-sized clusters have been utilized in solid-state lighting applications;[28] however, fundamental knowledge concerning their reactivity in aqueous media is limited.

Whereas numerous reports have focused on syntheses of cadmium chalcogenide NCs,[3,29] comparatively fewer have focused on their reactivity after removal from the reaction mixture. Nonetheless, a comprehensive understanding of the physical and chemical properties associated with reactivity of NCs as well as the kinetics and mechanisms of their degradation is required to optimize NCs for various applications. The postsynthesis degradation of cadmium chalcogenide NCs capped with thiols and phosphine oxides has often been attributed to surface oxidation and the loss of capping ligands.[30−36] The resulting release of free Cd^{2+} into solution has also been correlated with cytotoxicity.[37−40] Various reports have focused on the influence of solution pH,[30,35] ionic strength,[35,36] and the presence of potential ligands[31−35] on the reactivity of NCs. These reports stress that unreactive

Received: May 10, 2011
Revised: June 28, 2011
Published: July 15, 2011

metal−ligand bonds at the surfaces of NCs are correlated with the resistance of NCs to degradation.

In contrast, a few reports have revealed that discrete cadmium−ligand complexes are formed upon dissolution of NCs, suggesting that the degradation of NCs can be driven by the formation of metal−ligand complexes. For example, in 1998, Ptatschek et al. reported dramatic changes in the optical properties of magic-sized NCs upon exposure to alkylphosphine and amine ligands.[41] The changes were correlated with the formation of Cd^{2+}−ligand complexes. More recently, Siy and Bartl demonstrated that the degradation of certain NCs was associated with the formation of metal−ligand complexes and that NCs remained in suspension when present in equilibrium with their molecular precursors.[42]

This manuscript reports on the temporal persistence of magic-sized Cys-capped CdSe NCs after removal from the reaction mixture. The NCs are prepared via a straightforward all-aqueous route and exhibit very narrow absorption spectral features. The NCs persist on long time scales (90 days) in the reaction mixtures from which they are synthesized.[17] Thus, they are appealing for fundamental studies and for a range of applications that require water-dispersible materials. We present a systematic evaluation of the temporal persistence of the NCs after removal from the original reaction mixture and dilution into aqueous media. Notably, the CdSe NCs persisted only in the presence of a particular molecular Cd^{2+}−Cys complex. Otherwise, the NCs degraded through either of two pathways, the relative contributions of which varied with the composition of the aqueous medium. Our results highlight the influence of complex-formation equilibria on the temporal persistence of cadmium chalcogenide NCs in aqueous dispersions.

EXPERIMENTAL SECTION

CdSe NCs were synthesized by adaptation of a reported procedure.[16−18] Briefly, a selenide precursor was made by combining Se (0.167 g) and $NaSO_3$ (0.797 g) in deionized water (DI) (42 mL) in a round-bottomed flask that was covered in foil and allowed to reflux overnight. An aliquot from the selenide precursor solution (4 mL) was added to a stirred cadmium precursor solution that contained Cys (0.180 g) and $3CdSO_4{\bullet}8H_2O$ (0.115 g) in DI (78 mL). The reaction mixture was allowed to age for 7 days in the dark prior to analysis. Samples of CdSe NCs were prepared for analysis by mixing equal volumes of 2-propanol and the CdSe reaction mixture. CdSe precipitated quickly, while unreacted precursors remained in solution. After centrifugation and removal of supernatant, CdSe NCs were isolated as a solid pellet and were reconstituted in NaOH (100 mM). An aliquot of this suspension (200 μL) was combined with an aliquot of a basic solution containing Cys and/or Cd^{2+} (2.8 mL) and placed into a sealed, plastic cuvette (1 cm path length). Absorption spectra were acquired with an Agilent 8453 UV−visible absorption spectrophotometer. X-ray powder diffraction data were obtained with a Rigaku Ultima IV X-ray diffractometer. A more detailed experimental procedure can be found in the Supporting Information.

RESULTS AND DISCUSSION

Synthesis and Characterization of Cys-capped CdSe NCs. NCs were prepared following the method of Park et al. by combining Cys, $CdSO_4$, and $NaSeSO_3$ in a pH 12.5 aqueous solution.[16−18] Reaction mixtures were aged under ambient conditions in the dark for 7 days, yielding yellow suspensions with narrow absorption bands centered at 422, 391, and 362 nm (Figure S1 of the Supporting Information). The spectra of as-synthesized CdSe NCs are consistent with those reported by Park et al.[16] The wavelength at the maximum of the first excitonic band (λ_{max}) was 422 nm, and its full-width at half-maximum (fwhm) was 17 nm (960 cm^{-1}). The first excitonic band was approximately 3-fold more intense than the band centered at 362 nm. The high energy, high intensity, and narrow bandwidth of the first excitonic transition differ from those of regular quantum dots with distributions of particle sizes[6,43,44] and are instead consistent with the formation of monodisperse magic-sized clusters.[16,41,45−47] The absorption spectra of the as-synthesized NCs closely resemble those of previously reported $Cd_{33}Se_{33}$ or $Cd_{34}Se_{34}$ clusters.[16,45] On the basis of mass spectrometry measurements and theoretical modeling, Kasuya et al. described these clusters as consisting of a $(CdSe)_5$ or $(CdSe)_6$ core encapsulated by a $(CdSe)_{28}$ puckered cage, with approximately 82−85% of the atoms on the surface.[45] Using an empirically derived expression relating λ_{max} to the size of CdSe NCs,[48] we estimated the diameter of our NCs to be ∼1.7 nm. X-ray powder diffraction (XRD) data of the as-synthesized CdSe NCs (Figure S2 of the Supporting Information) consisted of bands centered at 2θ values of 27° (fwhm of 6.8°) and 45° (fwhm of 7.7°). The diffraction peaks were less well-resolved and significantly broader than those of bulk wurtzite or zinc-blende CdSe. Murray et al. reported similarly broad XRD features centered at 28° and 45° for 1.2 nm diameter TOPO-capped CdSe NCs.[6] In summary, on the basis of their absorption spectra and diffraction patterns, we conclude that the as-synthesized CdSe NCs with λ_{max} of 422 nm were magic-sized clusters with diameters less than 2 nm. We hereafter refer to them as MC_{422}, an abbreviation for magic-sized clusters with λ_{max} of 422 nm.

Dilution of MC_{422} into Basic Aqueous Solution. Our analysis of the chemical fate of MC_{422} upon dispersion into aqueous solutions focused primarily on the temporal evolution of its first excitonic absorption band. Other components of the reaction mixtures, such as Cd^{2+}−Cys complexes and other molecular precursors, absorbed below 350 nm. Within approximately one week after aliquots of MC_{422} were extracted from the reaction mixture and dispersed into aqueous NaOH (100 mM) solutions, the absorption spectrum changed dramatically (Figure 1). The absorbance at the first excitonic maximum (A_{max}) decreased. A red-shifted band developed, indicating the formation of larger CdSe particles or clusters. The absorbance of the red-shifted band approached a maximum at ∼130 h. On longer time scales, excitonic transitions became broader and less intense, and a red solid eventually formed at the bottom of the cuvette. This solid could not be redispersed into aqueous NaOH (100 mM).

The rate at which A_{max} decreased varied inversely with the concentration of MC_{422}; A_{max} of the most dilute sample decreased most rapidly (Figure S3 of the Supporting Information). The value of λ_{max} was unchanged within the first 8 h after dilution into basic solution, suggesting that MC_{422} dissolved into molecular species that did not absorb visible light. The first excitonic band then blue-shifted to a final λ_{max} of ∼416 nm (Figure 1 and Figure S4 of the Supporting Information). The first excitonic band broadened asymmetrically while it decreased in intensity, with greater broadening at longer wavelengths. Asymmetric broadening is consistent with the formation of new lower-energy bands rather than a symmetric increase of the size distribution of NCs. The rate at which fwhm of the first excitonic band increased mirrored the rate at which

A_{max} decreased (Figure S5 of the Supporting Information). Four isosbestic points were observed during the change of the spectrum of MC_{422} (Figure 2), suggesting that larger CdSe NCs with red-shifted absorptions formed through quantized or discontinuous growth rather than continuous ripening.[41,49,50] Notably, Vossmeyer et al. observed discontinuous growth of CdS NCs when the cluster size was below a certain threshold.[50] Discontinuous growth of CdSe clusters has also been reported.[41,49]

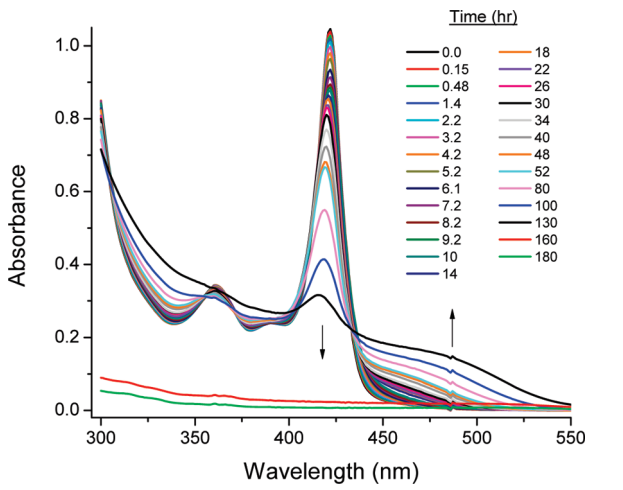

Figure 1. Temporal evolution of the absorption spectrum of MC_{422} after dilution into 100 mM NaOH. Arrows indicate the direction of the change of absorbance prior to the formation of a red solid.

The observed degradation of cadmium chalcogenide NCs upon dilution is not unprecedented. Döllefeld et al. reported that thiol-capped CdS NCs degraded upon purification and dilution into water.[51] Similarly, Kalyuzhny and Murray reported that CdSe NCs capped with TOPO and tri-*n*-octylphosphine selenide degraded after dilution into $CHCl_3$.[33] Degradation was attributed to the loss of surface ligand; the introduction of excess ligand into the NC-containing dispersion either halted or reversed the decay. The presence of excess ligands in aqueous suspensions of thiol-capped CdSe NCs has also been shown to prevent flocculation and to inhibit photooxidation.[30,31] In contrast, several groups have reported that the presence of free ligands can induce the degradation of NCs.[30,31,42] For example, Siy and Bartl recently reported that CdSe NCs capped with amines or carboxylic acids dissolved upon dilution into octadecylamine.[42] They measured an inverse relationship between the concentration of NCs and the rate of degradation, as demonstrated above for aqueous MC_{422}. In light of the conflicting reports in the literature pertaining to the influence of free ligand

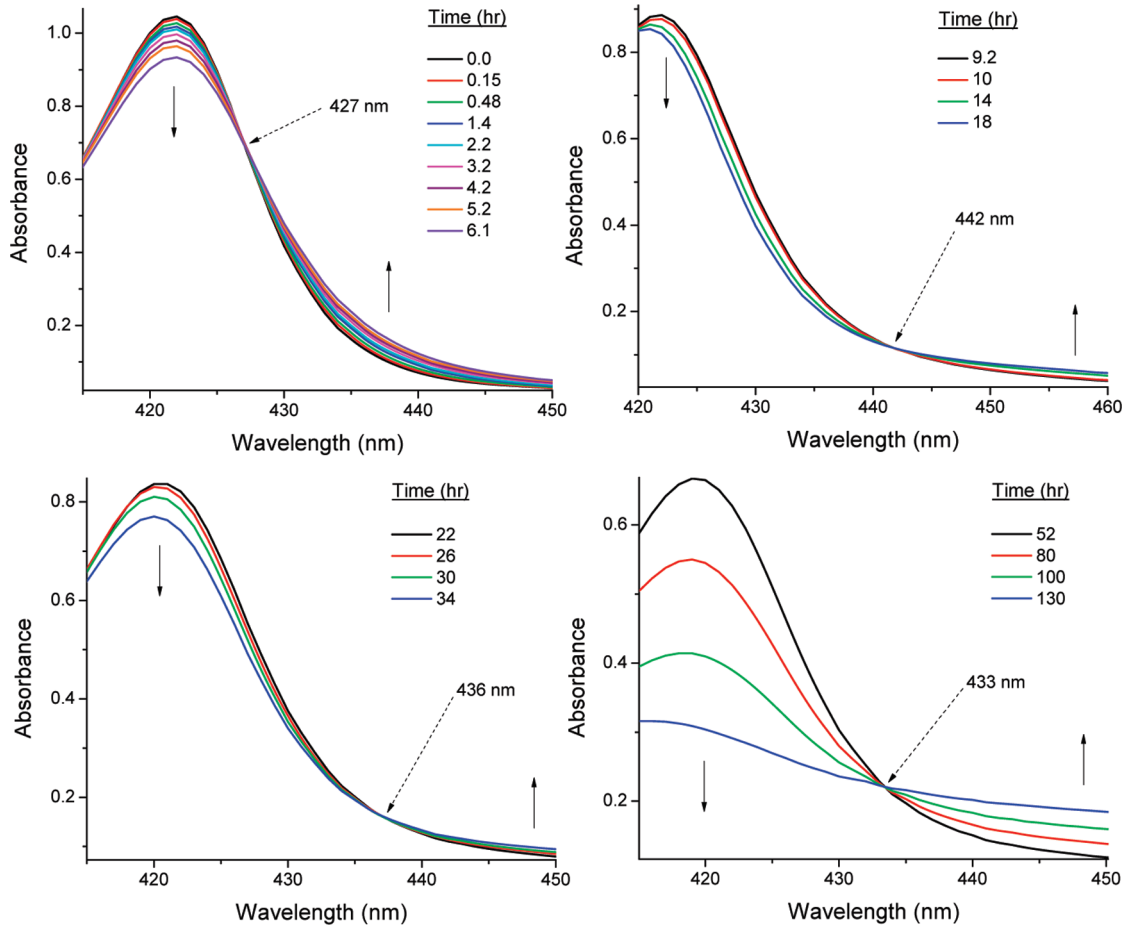

Figure 2. Absorption spectra measured at various times after dilution of MC_{422} into 100 mM NaOH; groups of spectra containing each of the four isosbestic points are presented together. Solid arrows indicate the direction of change in absorbance over time.

dx.doi.org/10.1021/cm2013347 |*Chem. Mater.* 2011, 23, 3546–3555

on the reactivity of NCs, we next characterized MC_{422} in the presence of varying concentrations of Cys.

Dilution of MC_{422} into Aqueous Solutions of Cys. Dilution of suspensions of MC_{422} into basic aqueous solutions containing 81 or 144 mM Cys resulted in a rapid decrease of the excitonic bands centered at 360 and 422 nm (Figure 3). Spectra did not contain isosbestic points or exhibit the growth of red-shifted absorption bands. No formation of red solid was discernible on long time scales. Thus, the mechanism by which MC_{422} degraded in the presence of high concentrations of Cys differed markedly from the mechanism of its degradation in the absence of Cys. MC_{422} degraded more rapidly in the presence of 144 mM Cys than in the presence of 81 mM Cys (Figure S6a of the Supporting Information). For both samples, the first excitonic transition of MC_{422} initially red-shifted to 425−426 nm, then blue-shifted to 420−422 nm (Figure S6b of the Supporting Information); the band then disappeared (Figure S6a of the Supporting Information). The final spectra contained broad bands centered at ∼380 nm with little contribution from the first excitonic band of MC_{422} (Figure 3). Absorption spectra of control solutions containing only $CdSO_4$ and Cys (but no MC_{422}) developed a similar band centered at ∼380 nm (Section S1 and Figure S7 of the Supporting Information). We speculate that the 380 nm absorption arose from formation of CdS NCs. Regardless, our data clearly indicate that MC_{422} degraded rapidly in solutions containing 144 mM or 81 mM Cys.

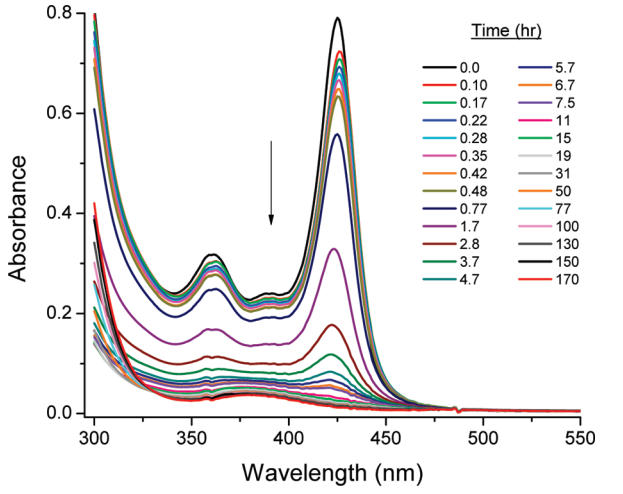

Figure 3. Temporal evolution of the absorption spectrum of MC_{422} after dilution into aqueous solutions containing 81 mM Cys (pH > 12.5). The arrow indicates the direction of the change of absorbance.

Dilution of MC_{422} into basic aqueous solutions with lower concentrations of Cys (1−18 mM) resulted in degradation of MC_{422} via a considerably different pathway (Figure 4a). On short time scales, the process corresponded closely to the degradation observed with higher concentrations of Cys; A_{max} decreased and λ_{max} red-shifted. After ∼5 h, however, A_{max} began to decrease more slowly and λ_{max} blue-shifted to a final value of ∼420 nm. At ∼50 h, A_{max} stabilized then increased, indicating the reformation of MC_{422} (Figure 4b). On long time scales (100−200 h), a red-shifted band developed, similar to the band that formed after dilution of MC_{422} into basic solutions without Cys (Figure 1).

In summary, the degradation of MC_{422} in the presence of low concentrations of Cys exhibited certain characteristics similar to degradation both in the absence of Cys and in the presence of high concentrations of Cys. The kinetics and extent of changes of A_{max} and λ_{max} were strongly influenced by the concentration of Cys (Figure S8 of the Supporting Information). A_{max} decreased more rapidly and λ_{max} red-shifted more significantly at higher concentrations of Cys. A_{max} stabilized (after the initial decrease) more rapidly at lower concentrations of Cys.

Dilution of MC_{422} into Aqueous Solutions of Cd^{2+} and Cys. Given the reactivity of MC_{422} in the presence of Cys, we next focused on the influence of Cd^{2+} on the kinetics and mechanism of degradation. Jalilehvand et al. recently described the speciation

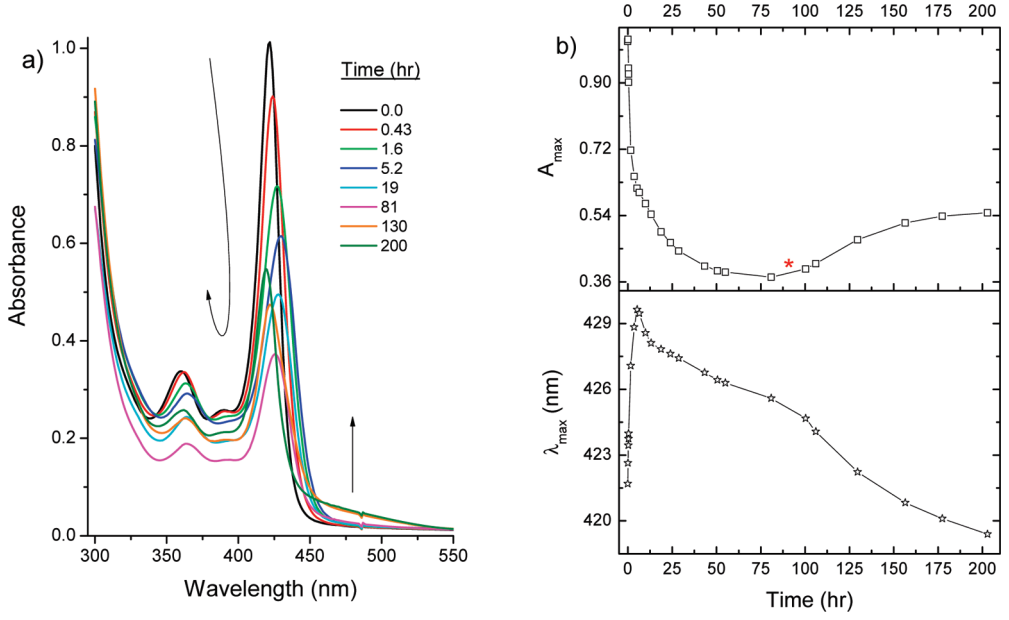

Figure 4. (a) Temporal evolution of the absorption spectrum of MC_{422} after dilution into an aqueous solution containing 18 mM Cys and 100 mM NaOH. Selected spectra are shown for clarity. Arrows indicate directions of the changes of absorbance. (b) A_{max} (top) and λ_{max} (bottom) as a function of time; the red asterisk (top trace) designates the time at which the red-shifted absorption band was first observed.

dx.doi.org/10.1021/cm2013347 |*Chem. Mater.* 2011, 23, 3546–3555

Scheme 1. Cd^{2+}—Cys Complex-Formation Equilibria in Basic Aqueous Solution

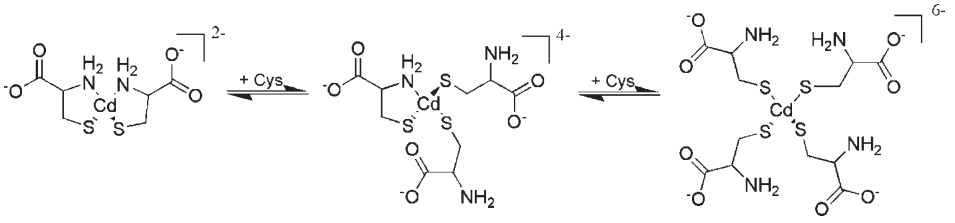

Table 1. Molar Ratios of Cys:Cd^{2+} (R) and Major Complexes Present in Solutions into which MC_{422} Was Diluted

solution	R	[Cys] (mM)	[Cd^{2+}] (mM)	predominant complex(es)
1	2.0	18	9.0	$[Cd(Cys)_2]^{2-}$
2	2.0	11	5.5	$[Cd(Cys)_2]^{2-}$
3	3.3	18	5.5	$[Cd(Cys)_2]^{2-}$ and $[Cd(Cys)_3]^{4-}$
4	6.5	18	2.8	$[Cd(Cys)_2]^{2-}$ and $[Cd(Cys)_3]^{4-}$
5	6.5	36	5.5	$[Cd(Cys)_2]^{2-}$ and $[Cd(Cys)_3]^{4-}$
6	13	18	1.4	$[Cd(Cys)_3]^{4-}$ and $[Cd(Cys)_4]^{6-}$
7	13	72	5.5	$[Cd(Cys)_3]^{4-}$ and $[Cd(Cys)_4]^{6-}$
8	26	18	0.69	$[Cd(Cys)_4]^{6-}$
9	26	144	5.5	$[Cd(Cys)_4]^{6-}$

of aqueous complexes of Cd^{2+} and Cys as a function of their relative concentrations and pH.[52] At a pH above the three pK_a values of Cys, relevant equilibria involve three mononuclear cadmium(II) complexes (Scheme 1).[52] Jalilehvand et al. demonstrated that the equilibrium concentrations of multinuclear Cd^{2+}—Cys complexes are negligible;[52] thus, we assume that only mononuclear complexes were present in solution. Because MC_{422} persisted for long time periods in the original reaction mixture containing 5.5 mM Cd^{2+} and 18 mM Cys, we diluted MC_{422} into solutions with Cys-to-Cd^{2+} molar ratios (R) greater than or less than 3.3 (Table 1). All solutions were basic with pH ≥ 12.5.

$R = 2$. Dilution of MC_{422} into either of two solutions with $R = 2$ (solutions 1 or 2, Table 1) led to rapid degradation of MC_{422}, yielding an absorption spectrum with few features in the visible (Figure 5). The spectral changes were very similar upon dilution of MC_{422} into solutions 1 and 2. This result, together with Jalilehvand's speciation data,[52] indicates that MC_{422} degraded in solutions containing $[Cd(Cys)_2]^{2-}$ as the predominant complex (Table 1). A_{max} decreased nonexponentially, suggesting that at least two processes contributed to the degradation of MC_{422} at short time scales (Figure S9 of the Supporting Information). Within the initial ~0.5 h after dilution, A_{max} decreased without any shifting of λ_{max} (Figure S9b of the Supporting Information). On longer time scales, a blue-shift of λ_{max} was correlated with the decrease of A_{max} (Figure S9a of the Supporting Information). After λ_{max} blue-shifted to ~416 nm, the band was no longer measurable. This degradation mechanism differed from the degradation mechanisms following dilution of MC_{422} into aqueous base, into Cys solutions without Cd^{2+} or into solutions in which Cd^{2+}—Cys complexes other than $[Cd(Cys)_2]^{2-}$ predominated.

R = 3.3, 6.5 and 13. MC_{422} exhibited excellent temporal persistence upon dilution into Cd^{2+}—Cys solutions with R values of 3.3, 6.5, and 13 (Figures 6 and 7). No shifting of λ_{max} or growth

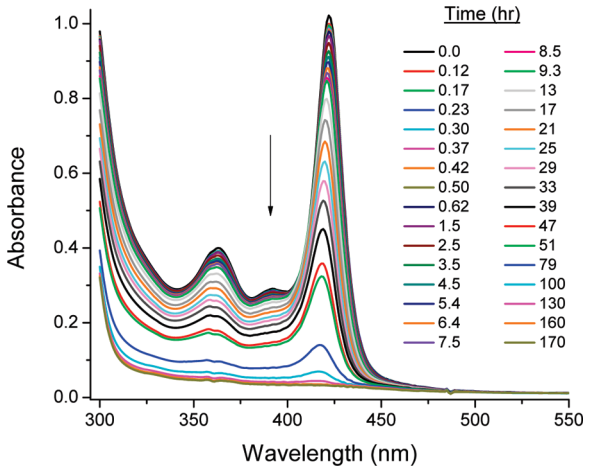

Figure 5. Temporal evolution of the absorption spectrum of MC_{422} after dilution into solution 1 ($R = 2$). The arrow indicates the direction of the change of absorbance.

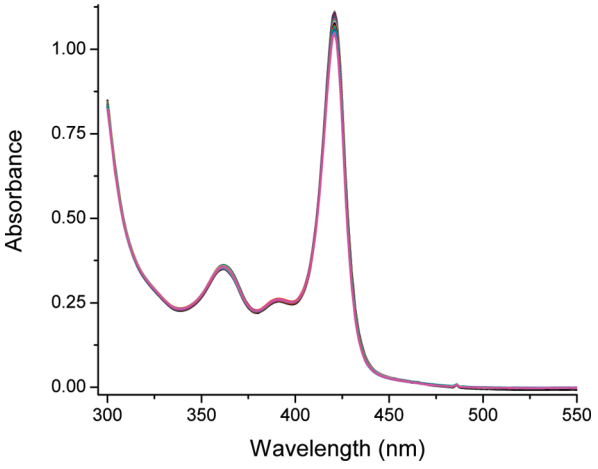

Figure 6. Temporal evolution of the absorption spectrum of MC_{422} after dilution into solution 3 ($R = 3.3$). Spectra were acquired for 170 h after dilution; 30 spectra are shown.

of new absorption bands occurred within one week of dilution of MC_{422} into such solutions. In solutions 4 and 5 ($R = 6.5$) and solutions 6 and 7 ($R = 13$), A_{max} of MC_{422} initially increased by 2—3%, then decreased slightly over the course of 7 days. In solution 3 ($R = 3.3$), A_{max} of MC_{422} increased by 0.6% within the first 6 min and decreased by ~5% within 7 days. MC_{422} was diluted into two different solutions (4 and 5) with R of 6.5 and two different solutions (6 and 7) with R of 13; for a given R value,

dx.doi.org/10.1021/cm2013347 |*Chem. Mater.* 2011, 23, 3546–3555

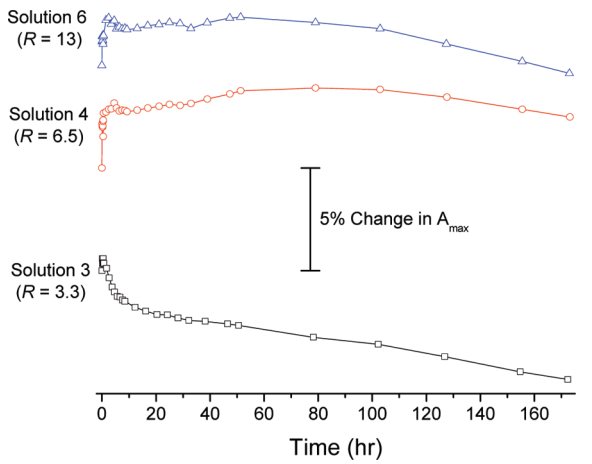

Figure 7. Normalized A_{max} values as a function of time after dilution of MC_{422} into solutions 3 (R = 3.3), 4 (R = 6.5), and 6 (R = 13). The scale bar indicates a 5% change of normalized A_{max}.

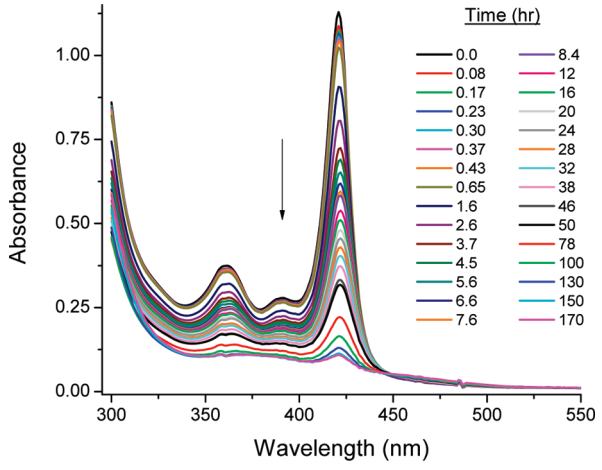

Figure 8. Temporal evolution of the absorption spectrum of MC_{422} after dilution into solution 9 (R = 26, $[Cd^{2+}]$ = 5.5 mM, [Cys] = 144 mM). Arrow indicates the direction of the change of absorbance.

the solutions differed in the concentrations of Cd^{2+} and Cys (Table 1). The temporal evolution of the absorption spectrum of MC_{422} depended only on the value of R and not on the concentrations of Cd^{2+} and Cys.

Jalilehvand's speciation data,[52] summarized in Table 1, suggest that $[Cd(Cys)_3]^{4-}$ was a predominant complex in Cd^{2+}—Cys solutions with R of 3.3, 6.5, and 13. Given the persistence of MC_{422} in such solutions, we propose that $[Cd(Cys)_3]^{4-}$ is a molecular precursor to MC_{422}. That is, MC_{422} and $[Cd(Cys)_3]^{4-}$ are in equilibrium, and the presence of a sufficient concentration of solvated $[Cd(Cys)_3]^{4-}$ prevents degradation of MC_{422}. Park et al. also concluded that $[Cd(Cys)_3]^{4-}$ is a precursor to MC_{422} by analysis of their synthetic results.[16] The reaction mixture in which MC_{422} is synthesized and persists has a Cys-to-Cd^{2+} molar ratio of 3.3.

R = 26. Dilution of MC_{422} into solutions 8 and 9 (R = 26, Table 1) led to different degradation pathways. MC_{422} degraded rapidly in solution 9 (Figure 8); absorption spectra initially evolved similarly to the spectra acquired upon dilution of MC_{422} into solutions containing 144 mM or 81 mM Cys alone (Figure 3). A_{max} decreased rapidly for approximately 30 min after

Scheme 2. Equilibria Describing the Formation and Degradation of MC_{422} in Aqueous Media with pH ≥ 12.5

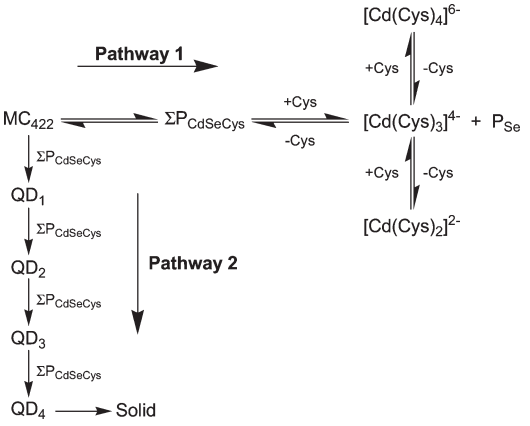

dilution, then decreased more slowly (Figure S10 of the Supporting Information). However, unlike degradation in solutions with high concentrations of Cys but without Cd^{2+}, the first excitonic band did not disappear within the analysis time (7 days). The value of λ_{max} varied only slightly, red-shifting by 1 nm within the initial 10 h, then returning more slowly to the initial value (Figure S10 of the Supporting Information). Finally, a red-shifted absorption band was measurable on long time scales. In contrast, MC_{422} did not degrade significantly after dilution into solution 8, with a lower concentration of Cd^{2+}, similar to its behavior upon dilution into solutions 3 through 7 (R = 3.3, 6.5 and 13). A_{max} decreased by only ~8% after 5 h, and λ_{max} did not shift (Figure S11 of the Supporting Information). Differences in the fate of MC_{422} after dilution into solutions 8 and 9 are discussed below.

Equilibria That Determine Persistence of MC_{422} and Degradation Pathway. We propose the equilibria in Scheme 2 to account for changes in the absorption spectrum of MC_{422} upon dilution into basic aqueous solutions containing Cd^{2+} and/or Cys at varying concentrations and molar ratios. The chemistry in Scheme 2 is predicated on several simplifying assumptions. First, we assume that the growth of MC_{422} from $[Cd(Cys)_3]^{4-}$ proceeded through a series of $Cd_xSe_yCys_z$ precursors, where $x,y,z \geq 1$. Such precursors are represented collectively as "$\Sigma P_{CdSeCys}$" in Scheme 2. Second, given the basicity of the solutions into which MC_{422} was diluted, we assume that Cd^{2+} was present exclusively in Cd^{2+}—Cys complexes, in MC_{422} or in $\Sigma P_{CdSeCys}$. ($Cd(OH)_2$ has a solubility product constant (K_{sp}) of 7.2×10^{-15} at 25 °C, and CdSe is insoluble in water. Thus, their concentrations were negligible.[53]) Third, we assume that each Cd^{2+} ion in MC_{422} was coordinated by three or four selenide ions and one or zero Cys ions, consistent with reported structures of magic-sized CdSe clusters including $Cd_{33}Se_{33}$ and $Cd_{34}Se_{34}$.[45] Thus, the molar ratio of Cys to Cd^{2+} in any of the Cd^{2+}—Cys complexes was greater than in $\Sigma P_{CdSeCys}$ or in MC_{422}. It follows that the formation of MC_{422} from $[Cd(Cys)_3]^{4-}$ involved the dissociation of at least three Cd^{2+}—Cys bonds and the liberation of at least two Cys ions. Notably, Bartl and co-workers also recently suggested that ligands are liberated upon association of precursors into larger NCs.[42] Fourth, we made the simplifying assumption that a generalized selenide precursor, represented as "P_{Se}" in Scheme 2, reacted with $[Cd(Cys)_3]^{4-}$ to yield $\Sigma P_{CdSeCys}$. The identity of P_{Se} is unknown to us and is currently

dx.doi.org/10.1021/cm2013347 |*Chem. Mater.* 2011, 23, 3546–3555

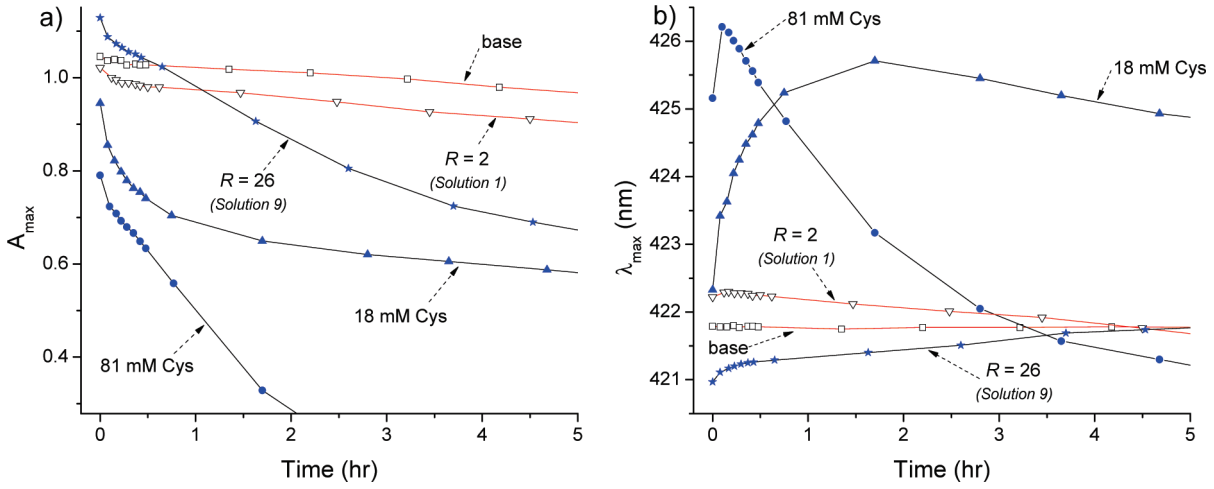

Figure 9. A_{max} (a) and λ_{max} (b) as a function of time after dilution of MC_{422} into aqueous solutions containing 100 mM NaOH and various concentrations of Cd^{2+} and/or Cys. The temporal evolution of both A_{max} and λ_{max} was similar in the absence of free Cys (red lines) or in the presence of excess uncoordinated Cys (black lines).

under investigation. Importantly, MC_{422} persisted after being diluted into solutions with R = 3.3, 6.5, and 13, which contained no P_{Se}. Finally, we neglected additional processes such as the oxidation of Cys to cystine and possible equilibria involving selenium and Cys.

Salient features of the chemistry proposed in Scheme 2 are as follows: (1) MC_{422} degrades via multiple pathways; (2) the presence or absence of free Cys in solution, together with the complex-formation equilibria involving Cd^{2+} and Cys (Scheme 1), determine whether MC_{422} persists and, if not, the pathway through which it degrades; and (3) MC_{422} persists in solutions that contain a sufficient concentration of $[Cd(Cys)_3]^{4-}$. The dependence of the degradation pathway and kinetics on the concentration of free Cys is clearly revealed by inspection of Figure 9, which shows the variation of A_{max} and λ_{max} within several hours after dilution of MC_{422} into solutions with free Cys (18 mM and 81 mM) and without free Cys (100 mM NaOH and solution 1 with R of 2). MC_{422} degraded slowly in solutions lacking free Cys, which we attribute to the absence of degradation via pathway 1 (Scheme 2). Although MC_{422} presumably degraded to yield some $\Sigma P_{CdSeCys}$, subsequent degradation to $[Cd(Cys)_3]^{4-}$ was precluded by the lack of free Cys in solution. In contrast, MC_{422} degraded rapidly in the presence of free Cys, as evidenced by decreased A_{max} and red-shifted λ_{max}, the rates of which increased with the concentration of Cys (Figure 9 and Figure S6 of the Supporting Information). This trend is consistent with the proposed chemistry in pathway 1 (Scheme 2), in which free Cys reacts with $P_{CdSeCys}$. In the following paragraphs, we revisit the degradation of MC_{422}, or the lack thereof, under various conditions within the context of the equilibria presented in Scheme 2.

We first consider the dilution of MC_{422} into 100 mM NaOH solutions that did not contain Cys. The growth of the broad and red-shifted absorption band after several days (Figure 1) is consistent with decay via pathway 2 (Scheme 2), which predominated in the absence of free Cys. We invoke the successive formation of four CdSe clusters and/or NCs (QD_{1-4} in Scheme 2) on the basis of the four isosbestic points that were measurable (Figure 2). During the time that each isosbestic point persisted, reaction mixtures contained MC_{422} and one of the larger clusters/NCs. Pathway 2 is presented without equilibrium notation as we do not speculate on the reversibility of the process. The insolubility of the red solid suggests irreversibility in the later stages of pathway 2.

We next consider dilution of MC_{422} into solutions of Cys with varying concentrations (1−144 mM). Because these solutions initially contained free Cys, MC_{422} initially degraded via pathway 1 (Scheme 2). The net loss of MC_{422} resulted primarily in the formation of $[Cd(Cys)_4]^{6-}$ (due to the high value of R[52]) and the associated decrease of A_{max} (Figures 3 and 4, Figures S6 and S8 of the Supporting Information). The initial rate of change of A_{max} increased with concentration of Cys (Figure S6 of the Supporting Information), indicating that degradation was non-zeroth order with respect to Cys. The influence of the concentration of Cys on the kinetics of degradation of MC_{422} provides compelling evidence that Cys is a reactant in pathway 1. Within 3−15 h after dilution of MC_{422} into 81 mM and 144 mM Cys, the concentration of intact MC_{422} was negligible (Figure 3 and Figure S6 of the Supporting Information), presumably because the vast majority of Cd^{2+} was present within solvated $[Cd(Cys)_4]^{6-}$.

The absorption spectral changes on long time scales after dilution of MC_{422} into the lower-concentration solutions of Cys (1−18 mM) were considerably more complex (Figure 4 and Figure S8 of the Supporting Information). These data clearly indicate that the concentration of free Cys determines the interplay between pathways 1 and 2 (Scheme 2). As free Cys was depleted and R decreased during the initial degradation via pathway 1, the relative solute mole fraction of $[Cd(Cys)_3]^{4-}$, the molecular precursor in equilibrium with MC_{422}, increased. At a sufficient concentration of $[Cd(Cys)_3]^{4-}$, there was no longer a net loss of MC_{422} via pathway 1, giving rise to the observed stabilization of A_{max} (Figure 4 and Figure S8 of the Supporting Information). A_{max} stabilized most rapidly after dilution of MC_{422} into 1 mM Cys and least rapidly after dilution into 18 mM Cys (Figure S8 of the Supporting Information). Remarkably, the concentration of MC_{422} began to increase three to four days after dilution into 9 and 18 mM solutions of Cys, as evidenced by the regrowth of the narrow first excitonic absorption band (Figure 4) and the corresponding increase of A_{max} (Figure 4 and Figure S8 of the Supporting Information).

dx.doi.org/10.1021/cm2013347 |Chem. Mater. 2011, 23, 3546–3555

This process began earlier for 9 mM Cys than for 18 mM Cys, which again suggests that the reformation of MC_{422} was triggered by the depletion of free Cys and the corresponding increase of the relative solute mole fraction of $[Cd(Cys)_3]^{4-}$. Eventually, the concentration of Cys decreased enough that MC_{422} began to decay via pathway 2, giving rise to the observed growth of the broad, red-shifted absorption bands associated with QD_{1-4} (Figure 4). The transition from pathway 1 to 2 occurred more rapidly at lower concentrations of Cys (Figure S8a of the Supporting Information). Taken together, these data reveal that the persistence or degradation of MC_{422} after dilution into basic solutions of Cys was dictated by the amount of free Cys and the relative solute mole fractions of the three Cd^{2+}-Cys complexes in solution, both of which depended on R. Thus, the data are consistent with the proposed equilibria in Scheme 2.

The extent to which MC_{422} degraded after dilution into solutions containing both Cd^{2+} and Cys varied greatly with R. MC_{422} persisted after dilution into Cd^{2+}−Cys solutions with R of 3.3, 6.5, and 13. The Cd^{2+}−Cys complex-formation equilibria (Scheme 1) favored $[Cd(Cys)_3]^{4-}$ as the predominant complex at these R values.[52] At sufficient concentrations of $[Cd(Cys)_3]^{4-}$, the equilibria of pathway 1 (Scheme 2) were shifted to the left; thus, the net loss of MC_{422} was minimal. Interestingly, A_{max} increased within the first several minutes after dilution of MC_{422} into solutions 4 (R = 6.5) and 6 (R = 13) (Figure 7). This surprising result can be explained in terms of the sample-preparation process. After MC_{422} was removed from the original reaction mixture, the flocculate was redispersed to an equal concentration in 100 mM NaOH prior to being diluted into the various solutions. During the time between redispersion and dilution, $\Sigma P_{CdSeCys}$ began to form via pathway 1 (Scheme 2). Thus, when the aliquot of MC_{422} was diluted into a solution already containing $[Cd(Cys)_3]^{4-}$, the equilibria of pathway 1 were shifted toward the formation of MC_{422}.

The fate of MC_{422} after dilution into solutions with R of 26 varied with the concentration of Cd^{2+} (Figure 8 and Figures S10 and S11 of the Supporting Information). We first consider solution 9, in which $[Cd(Cys)_4]^{6-}$ was most likely the predominant Cd^{2+}−Cys complex.[52] On short time scales after dilution of MC_{422} into solution 9, plots of A_{max} and λ_{max} versus time were similar in form to the corresponding plots obtained after dilution of MC_{422} into solutions of 81 or 144 mM Cys alone (Figure 9). However, the spectral changes occurred much more slowly after dilution of MC_{422} into solution 9 (Figure 9 and Figure S6 of the Supporting Information). On longer time scales, the presence of Cd^{2+} in solution 9 eventually led to appreciable degradation of MC_{422} via pathway 2, as evidenced by the growth of red-shifted absorption bands (Figure 8). In contrast, pathway 2 did not contribute significantly to the degradation of MC_{422} after dilution into 81 or 144 mM solutions of Cys. These differences can be attributed to the influence of R on the Cd^{2+}−Cys complex-formation equilibria (Scheme 1) and the influence of free Cys on the relative contributions of pathways 1 and 2 (Scheme 2). The slower initial rate of degradation of MC_{422} via pathway 1 after dilution into solution 9 is consistent with the decreased concentration of free Cys, due to the formation of Cd^{2+}−Cys complexes (Scheme 1). On long time scales, the concentration of Cys was apparently sufficiently depleted, through coordination to Cd^{2+} originally present in solution 9 and generated via degradation of MC_{422}, that degradation via pathway 2 became significant.

MC_{422} persisted after being diluted into solution 8 (Figure S11 of the Supporting Information), which represents an 8-fold dilution of solution 9. The Cd^{2+}−Cys complex-formation equilibria (Scheme 1) were shifted further left for solution 8 than for solution 9; therefore, the relative solute mole fraction of $[Cd(Cys)_3]^{4-}$ was higher in solution 8 than in solution 9. Our data indicate that the concentration of $[Cd(Cys)_3]^{4-}$ was sufficiently high to prevent the net loss of MC_{422} via pathway 1. The vastly different behavior of MC_{422} after dilution into solutions 8 and 9 provides further evidence that Cd^{2+}−Cys complex-formation equilibria greatly influenced the mechanism and extent of degradation of MC_{422}.

Finally, we consider the dilution of MC_{422} into Cd^{2+}−Cys solutions 1 and 2 (R = 2). To a first approximation, Cd^{2+} was present exclusively within $[Cd(Cys)_2]^{2-}$, and the solutions contained no free Cys. Thus, reaction via pathway 2 was anticipated, similar to the reactivity of MC_{422} after dilution into 100 mM NaOH solutions without Cys. Indeed, within the first several hours, absorption spectral data for MC_{422} in solution 1 and in 100 mM NaOH were nearly superimposable (Figure 9): the decrease of A_{max} and the red-shift of λ_{max} were negligible (Figures 5, 9). On long time scales after dilution of MC_{422} into solution 1 or 2, however, there was no evidence for degradation of MC_{422} via pathway 2 and the formation of QD_{1-4}. We speculate that $[Cd(Cys)_2]^{2-}$ inhibited the formation of QD_{1-4}, possibly through interaction with $\Sigma P_{CdSeCys}$. However, we are unsure of the nature of inhibition or of the interaction between $[Cd(Cys)_2]^{2-}$ and $\Sigma P_{CdSeCys}$.

Perturbation of the Equilibria. We performed two additional experiments to investigate further the influence of the equilibria presented in Scheme 2 on the reactivity of MC_{422}. The experiments are described in detail in Section S1 of the Supporting Information. First, an aliquot was removed from the original reaction mixture containing as-synthesized MC_{422} and its precursors. MC_{422} was not flocculated by the addition of 2-propanol, as it was in each of the experiments described above. The aliquot was then dispersed into 100 mM NaOH, which gave rise to a slow decrease of A_{max} of MC_{422} (Figure S12 of the Supporting Information). Importantly, A_{max} decreased much more slowly and to a lesser extent during this experiment than following the dilution of flocculated MC_{422}, *which had been removed from the original reaction mixture*, into 100 mM NaOH (Figure 1 and Figure S3 of the Supporting Information). The difference in degradation kinetics provides additional evidence that $[Cd(Cys)_3]^{4-}$ is the molecular precursor to MC_{422} and prevents its net loss via pathway 1.

In the second experiment, an aliquot of the original reaction mixture was again diluted into 100 mM NaOH, without flocculation, then divided into multiple samples. Equilibria were perturbed by spiking the MC_{422}-containing samples with either $[Cd(Cys)_2]^{2-}$ or free Cys. The addition of $[Cd(Cys)_2]^{2-}$ to a concentration of 5.5 mM resulted in a rapid decrease of A_{max} (Figure 10a). Degradation kinetics closely resembled those measured following the dilution of *flocculated* MC_{422} into Cd^{2+}−Cys solutions 1 and 2 with R values of 2, which also contained $[Cd(Cys)_2]^{2-}$ (Figure S9 of the Supporting Information). Similarly, addition of free Cys to a concentration of 81 mM caused a rapid decrease of A_{max} (Figure 10b). In both experiments, perturbation of the Cd^{2+}−Cys complex-formation equilibria (Scheme 1) led to a decrease of the relative solute mole fraction of $[Cd(Cys)_3]^{4-}$ and a corresponding rapid and significant net loss of MC_{422}. This behavior is consistent with the chemistry proposed in Scheme 2.

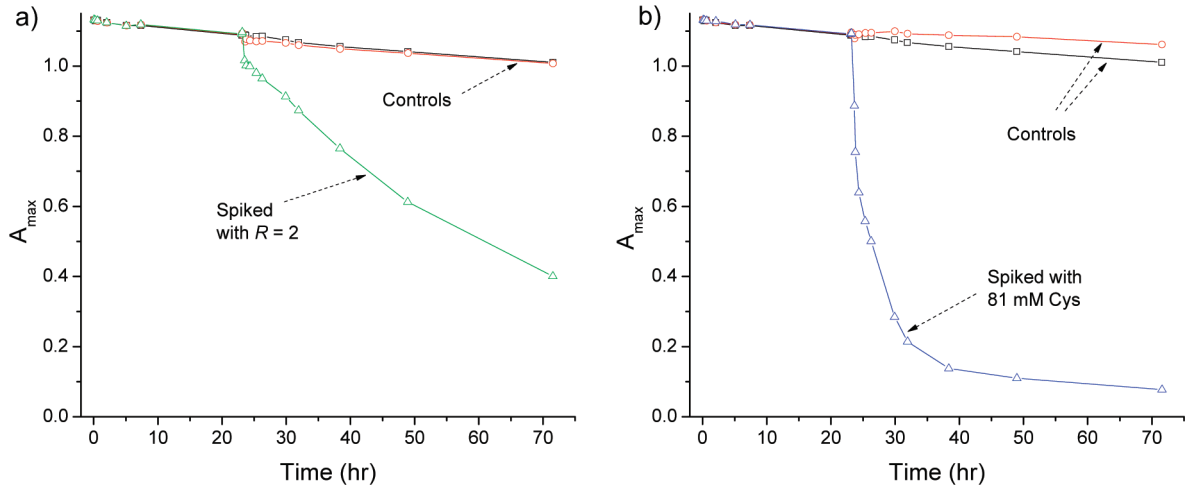

Figure 10. Temporal evolution of A_{max} for suspensions of MC_{422} taken directly from the original reaction mixture and spiked with a solution containing Cd^{2+} and Cys with R of 2 (a) and a large molar excess of free Cys (81 mM) (b). Controls are described in Section S1 of the Supporting Information.

CONCLUSIONS

Our results provide clear evidence that the reported stability of as-synthesized MC_{422} arises from its persistence in the original reaction mixture due to the presence of $[Cd(Cys)_3]^{4-}$. Our data also indicate that MC_{422} does not persist in the absence of $[Cd(Cys)_3]^{4-}$, either upon removal from the original reaction mixture or upon perturbation of the Cd^{2+}–Cys complex-formation equilibria in the reaction mixture. Under conditions in which MC_{422} does not persist, the presence or absence of free, uncoordinated Cys determines the degradation pathway. Our results highlight the importance of evaluating the postsynthetic reactivity of metal–chalcogenide NCs as a function of their composition, capping-group functionality, reactivity of the metal cation with free capping-group ligands, and the solvent in which they are dispersed.

More generally, our findings indicate that simply removing NCs from the reaction mixtures in which they were synthesized can induce degradation. Chemistry in the surrounding solution, in addition to chemistry occurring at the surfaces of NCs, can dramatically alter the temporal persistence of NCs and the kinetics and mechanism of their degradation. The reactivity and persistence of NCs have tremendous influence on their utility and potential applications; therefore, mechanisms leading to the degradation of NCs must be considered carefully and warrant continued investigation.

ASSOCIATED CONTENT

Supporting Information. S1: Experimental details and Table S1. S2: Figures S1–S12, which include absorption spectra and XRD data of as-synthesized MC_{422} as well as plots of A_{max} and λ_{max} as a function of time after dilution of MC_{422} into various aqueous media. This material is available free of charge via the Internet at http://pubs.acs.org.

AUTHOR INFORMATION

Corresponding Author

*E-mails: dwatson3@buffalo.edu (D.F.W.), lacolon@buffalo.edu (L.A.C.).

ACKNOWLEDGMENT

The authors acknowledge the financial support provided by the National Science Foundation, USA (CHE-1058373 and CHE-0645678). J.S.B. acknowledges the financial support provided by the Silbert Fellowship in Chemistry, Department of Chemistry, The State University of New York at Buffalo.

REFERENCES

(1) Biju, V.; Itoh, T.; Anas, A.; Sujith, A.; Ishikawa, M. *Anal. Bioanal. Chem.* **2008**, *391*, 2469.
(2) Sperling, R. A.; Parak, W. J. *Phil. Trans. R. Soc. A* **2010**, *368*, 1333.
(3) Gaponik, N.; Hickey, S. G.; Dorfs, D.; Rogach, A. L.; Eychmüller, A. *Small* **2010**, *6*, 1364.
(4) Kamat, P. V. *J. Phys. Chem. C* **2008**, *112*, 18737.
(5) Green, M. *J. Mater. Chem.* **2010**, *20*, 5797.
(6) Murray, C. B.; Norris, D. J.; Bawendi, M. G. *J. Am. Chem. Soc.* **1993**, *115*, 8706.
(7) Qu, L.; Peng, Z. A.; Peng, X. *Nano Lett.* **2001**, *1*, 333.
(8) Kuno, M.; Lee, J. K.; Dabbousi, B. O.; Mikulec, F. V.; Bawendi, M. G. *J. Chem. Phys.* **1997**, *106*, 9869.
(9) Chen, X.; Hutchison, J. L.; Dobson, P. J.; Wakefield, G. *J. Colloid Interface Sci.* **2008**, *319*, 140.
(10) Chu, M.; Shen, X.; Liu, G. *Nanotechnology* **2006**, *17*, 444.
(11) Huang, F.; Chen, G. *Spectrochim. Acta, Part A* **2008**, *70*, 318.
(12) Kalasad, M. N.; Rabinal, M. K.; Mulimani, B. G. *Langmuir* **2009**, *25*, 12729.
(13) Liu, H.; Owen, J. S.; Alivisatos, A. P. *J. Am. Chem. Soc.* **2006**, *129*, 305.
(14) Liu, P.; Wang, Q.; Li, X. *J. Phys. Chem. C* **2009**, *113*, 7670.
(15) Oluwafemi, S. O.; Revaprasadu, N.; Ramirez, A. J. *J. Cryst. Growth* **2008**, *310*, 3230.
(16) Park, Y.-S.; Dmytruk, A.; Dmitruk, I.; Kasuya, A.; Okamoto, Y.; Kaji, N.; Tokeshi, M.; Baba, Y. *J. Phys. Chem. C* **2010**, *114*, 18834.
(17) Park, Y.-S.; Dmytruk, A.; Dmitruk, I.; Kasuya, A.; Takeda, M.; Ohuchi, N.; Okamoto, Y.; Kaji, N.; Tokeshi, M.; Baba, Y. *ACS Nano* **2009**, *4*, 121.
(18) Park, Y.-S.; Dmytruk, A.; Dmitruk, I.; Yasuto, N.; Kasuya, A.; Takeda, M.; Ohuchi, N. *J. Nanosci. Nanotechnol.* **2007**, *7*, 3750.
(19) Raevskaya, A.; Stroyuk, A.; Kuchmii, S. *Theor. Exp. Chem.* **2006**, *42*, 113.
(20) Rogach, A. L.; Kornowski, A.; Gao, M.; Eychmuller, A.; Weller, H. *J. Phys. Chem. B* **1999**, *103*, 3065.
(21) Singh, S.; Rath, M. C.; Singh, A. K.; Sarkar, S. K.; Mukherjee, T. *Mater. Chem. Phys.* **2010**, *124*, 6.

(22) Song, L.; Duan, J.; Zhan, J. *Mater. Lett.* **2010**, *64*, 1843.
(23) Song, L.; Duan, J.; Zhan, J. *Chem. Lett.* **2010**, *39*, 942.
(24) Xia, Y.-S.; Zhu, C.-Q. *Mater. Lett.* **2008**, *62*, 2103.
(25) Yang, Y. J.; Xiang, B. J. *J. Cryst. Growth* **2005**, *284*, 453.
(26) Zhou, X.; Kobayashi, Y.; Ohuchi, N.; Takeda, M.; Kasuya, A. *Int. J. Mod. Phys. B* **2005**, *19*, 2835.
(27) Zhou, X.; Kobayashi, Y.; Romanyuk, V.; Ochuchi, N.; Takeda, M.; Tsunekawa, S.; Kasuya, A. *Appl. Surf. Sci.* **2005**, *242*, 281.
(28) McBride, J. R.; Dukes Iii, A. D.; Schreuder, M. A.; Rosenthal, S. J. *Chem. Phys. Lett.* **2010**, *498*, 1.
(29) Murray, C. B.; Kagan, C. R.; Bawendi, M. G. *Annu. Rev. Mater. Sci.* **2000**, *30*, 545.
(30) Aldana, J.; Lavelle, N.; Wang, Y.; Peng, X. *J. Am. Chem. Soc.* **2005**, *127*, 2496.
(31) Aldana, J.; Wang, Y. A.; Peng, X. *J. Am. Chem. Soc.* **2001**, *123*, 8844.
(32) Gaunt, J. A.; Knight, A. E.; Windsor, S. A.; Chechik, V. *J. Colloid Interface Sci.* **2005**, *290*, 437.
(33) Kalyuzhny, G.; Murray, R. W. *J. Phys. Chem. B* **2005**, *109*, 7012.
(34) Landes, C.; Braun, M.; Burda, C.; El-Sayed, M. A. *Nano Lett.* **2001**, *1*, 667.
(35) Mulvihill, M. J.; Habas, S. E.; Jen-La Plante, I.; Wan, J.; Mokari, T. *Chem. Mater.* **2010**, *22*, 5251.
(36) Noh, M.; Kim, T.; Lee, H.; Kim, C.-K.; Joo, S.-W.; Lee, K. *Colloids Surf., A* **2010**, *359*, 39.
(37) Derfus, A. M.; Chan, W. C. W.; Bhatia, S. N. *Nano Lett.* **2003**, *4*, 11.
(38) Kirchner, C.; Liedl, T.; Kudera, S.; Pellegrino, T.; Muñoz Javier, A.; Gaub, H. E.; Stölzle, S.; Fertig, N.; Parak, W. J. *Nano Lett.* **2004**, *5*, 331.
(39) Kloepfer, J. A.; Mielke, R. E.; Wong, M. S.; Nealson, K. H.; Stucky, G.; Nadeau, J. L. *Appl. Environ. Microbiol.* **2003**, *69*, 4205.
(40) Pace, H. E.; Lesher, E. K.; Ranville, J. F. *Environ. Toxicol. Chem.* **2010**, *29*, 1338.
(41) Ptatschek, V.; Schmidt, T.; Lerch, M.; Muller, G.; Spanhel, L.; Emmerling, A.; Fricke, J.; Foitzik, A. H.; Langer, E. *Ber. Bunsenges. Phys. Chem.* **1998**, *102*, 85.
(42) Siy, J. T.; Bartl, M. H. *Chem. Mater.* **2010**, *22*, 5973.
(43) Katari, J. E. B.; Colvin, V. L.; Alivisatos, A. P. *J. Phys. Chem.* **1994**, *98*, 4109.
(44) Peng, Z. A.; Peng, X. *J. Am. Chem. Soc.* **2000**, *123*, 183.
(45) Kasuya, A.; Sivamohan, R.; Barnakov, Y. A.; Dmitruk, I. M.; Nirasawa, T.; Romanyuk, V. R.; Kumar, V.; Mamykin, S. V.; Tohji, K.; Jeyadevan, B.; Shinoda, K.; Kudo, T.; Terasaki, O.; Liu, Z.; Belosludov, R. V.; Sundararajan, V.; Kawazoe, Y. *Nat. Mater.* **2004**, *3*, 99.
(46) Soloviev, V. N.; Eichhöfer, A.; Fenske, D.; Banin, U. *J. Am. Chem. Soc.* **2001**, *123*, 2354.
(47) Yu, K.; Hu, M. Z.; Wang, R.; Piolet, M. l. L.; Frotey, M.; Zaman, M. B.; Wu, X.; Leek, D. M.; Tao, Y.; Wilkinson, D.; Li, C. *J. Phys. Chem. C* **2010**, *114*, 3329.
(48) Yu, W. W.; Qu, L.; Guo, W.; Peng, X. *Chem. Mater.* **2003**, *15*, 2854.
(49) Kudera, S.; Zanella, M.; Giannini, C.; Rizzo, A.; Li, Y.; Gigli, G.; Cingolani, R.; Ciccarella, G.; Spahl, W.; Parak, W. J.; Manna, L. *Adv. Mater.* **2007**, *19*, 548.
(50) Vossmeyer, T.; Katsikas, L.; Giersig, M.; Popovic, I. G.; Diesner, K.; Chemseddine, A.; Eychmueller, A.; Weller, H. *J. Phys. Chem.* **1994**, *98*, 7665.
(51) Dollefeld, H.; Hoppe, K.; Kolny, J.; Schilling, K.; Weller, H.; Eychmuller, A. *Phys. Chem. Chem. Phys.* **2002**, *4*, 4747.
(52) Jalilehvand, F.; Leung, B. O.; Mah, V. *Inorg. Chem.* **2009**, *48*, 5758.
(53) *CRC Handbook of Chemistry and Physics*; 91st ed.; Haynes, W. M., Ed.; CRC Press: Boca Raton, FL, 2010.